Korean J. of Chem. Eng., **14**(4), 292-296 (1997)

MEASUREMENT AND CORRELATION OF SOLUBILITIES OF *o*-, *m*- AND *p*-COUMARIC ACID ISOMERS IN SUPERCRITICAL CARBON DIOXIDE

Eun Sun Choi, Hun Yong Shin, Seong-Sik You and Ki-Pung Yoo†

Department of Chemical Engineering, Sogang University, C.P.O. Box 1142, Seoul, Korea

(Received 30 April 1997 • accepted 31 July 1997)

Abstract – The solubility of isomeric *o*-, *m*- and *p*-coumaric acids in supercritical carbon dioxide were measured by a flow-type experimental apparatus at 308.15-323.15 K and 8.5-25 MPa. The data were modeled by an empirical density-based correlation and a recent EOS formulated by the authors based on approximated lattice-hole theory. We found that *m*-coumaric acid showed the highest solubility and *o*-coumaric acid showed the lowest solubility at the experimental pressures and temperatures.

Key words: *Supercritical Fluid Extraction, Carbon Dioxide, Biosubstances Coumaric Acid Isomers, Thermodynamic Modeling*

INTRODUCTION

Recently the supercritical fluid extraction (SFE) technology has been widely applied to obtain various pharmaceutical extracts and purified substances from natural products [Choi et al., 1996; Noh et al., 1997]. In general, an extract from a natural product by SFE contains various bioactive substances and their derivatives as well as isomers. For example, when one intends to isolate coumaric acid for pharmaceutical use from a target natural plant [i.e., *Morus alba*], there exist several isomers [i.e., *o*-, *m*-, and *p*-coumaric acid, etc.], as well as numerous coumarin derivatives in the extract [Noh et al., 1997]. Thus, to obtain a high-purity coumaric acid, it is of importance to know the solubility of existing isomeric coumaric acids in the supercritical fluid. However, no experimental data are available in the literature to date.

In the present study, three types of coumaric acid isomers were chosen and we quantitatively measured the solubility of coumaric acids in supercritical carbon dioxide. Since pure component properties necessary for thermodynamic modeling phase equilibria of coumaric acids are not well known, it would have been extremely difficult to use equation of state (EOS) for thermodynamic correlation. Thus, in this work, modeling phase equilibria of coumaric acids in supercritical fluid is reported by employing an empirical density model-based correlation [Li et al., 1991; Skerget et al., 1995] and an EOS developed recently by the present authors [Lee and Yoo, 1997].

EXPERIMENTAL

1. Reagents and Apparatus

Coumaric acids were purchased from Sigma Chem. Co. (<98 %, USA), and CO_2 (<99.9 %) was purchased from the Seoul Gas Co. (Seoul, Korea). A flow-type micro-scale phase equilibrium apparatus, as described in detail by Choi et al., 1996, was used. The apparatus was immersed in an air-bath installed with a PID temperature controller. CO_2 was transferred into an equilibrium cell (60 ml internal volume) using a syringe pump (ISCO 260 DM, USA), and pressure was measured by a Heise gauge (MM-43776, USA). The equilibrated effluent was passed through two-step methanol-filled traps and metering valves. The experiment was repeated three times for each sample solute.

2. HPLC Analysis

Separated solute was dissolved by methanol in the cold-trap. This dissolved solute was depressurized and diluted further with additional methanol and analyzed by HPLC (Milton Roy, USA). The column was YMC pack, ODS-A (250×4.6 mm, s-5 μm), with detection by UV 280 nm [Casteele et al., 1983]. The calibration results of HPLC analysis for *o*-, *m*- and *p*-coumaric acid are shown in Table 1. A regression curve for *o*-coumaric acid is shown in Fig. 1.

THERMODYNAMIC MODELING

1. Density Model-Based Correlation

In the first place, a density model-based correlation was tested to model the solubility data obtained in the present study [Giddings et al., 1969]. The model is given by

$$\log E=A+B\rho_1 \tag{1}$$

where ρ_1 is the density of solvent. E is an enhancement fac-

Table 1. Calibrated results for HPLC analysis for *o*-, *m*-, and *p*-coumaric acids

Solute	Concentration[mg/ml]=$b_1\times$HPLC Area+b_0		
	$b_1\times10^9$	$b_0\times10^4$	γ^2
o-coumaric acid	9.1492	0.66053	0.9997
m-coumaric acid	6.3136	1.4095	0.9960
p-coumaric acid	6.2819	11.6390	0.9968

---

†To whom all correspondence should be addressed.

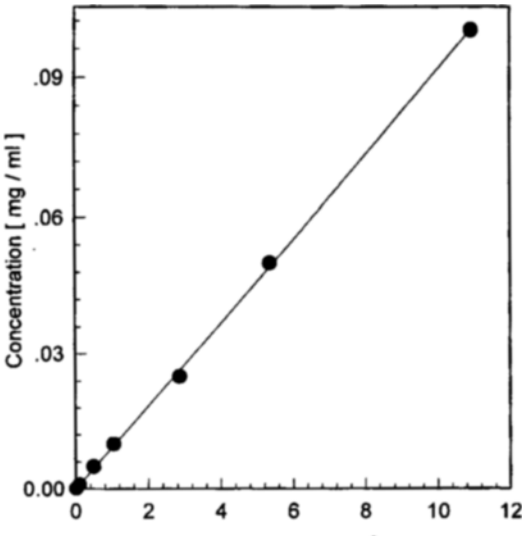

Fig. 1. Sample regression curve of *o*-coumaric acid for HPLC analysis.

Table 2. Best-fitted coefficients A and B in Eq. (1)

Solute	T [K]	A	B×10^3	γ^2	error
o-coumaric acid	308.15	−4.009	5.170	0.978	11.39
	313.15	−3.740	5.146	0.988	11.15
	323.15	−2.892	4.687	0.994	16.21
m-coumaric acid	308.15	−3.103	4.638	0.983	10.03
	313.15	−3.400	5.257	0.992	8.99
	323.15	−13.954	4.088	0.990	12.62
p-coumaric acid	308.15	−3.457	4.557	0.992	5.71
	313.15	−4.587	6.216	0.999	3.82
	323.15	−2.981	4.778	0.998	6.73

tor defined by Py_2/P_2^{sat} (y_2 is the mole fraction of a solute and P_2^{sat} is the vapor pressure of a solute set by 1 Pa).

The best fit of parameters A and B, and error range for each coumaric acid is given in Table 2.

2. Pure Physical Properties Estimation

As with most other natural bioactive substances, there is almost no information on the pure physical constants reported in literature for coumaric acids. Thus, the pure physical properties necessary for phase equilibria modeling of mixtures containing biosubstances have to based on a type of estimation method. Illustratively, we tried to employ the existing semi-empirical estimation methods for pure constants for calculating those physical properties constants [Lyman et al., 1990]. From this reference, the Lyderson-Forman-Thodos method for boiling point (T_b) and critical temperature (T_c) and the Miller method for critical pressure (P_c), critical volume (V_c), critical compressibility factor (Z_c) and acentric factor (ω) were used. The molar volumes and vapor pressures were estimated using the Bhirud method and Lee-Kestler correlation, respectively [Reid et al., 1987]. The estimated pure property constants for coumaric acids are summarized in Table 3 and 4.

Table 3. Estimated pure property constants of *o*-, *m*-, and *p*-coumaric acids

Solute	Pure physical properties					
	T_b [K]	T_c [K]	P_c [bar]	V_c [g/mol]	Z_c	ω
o-coumaric acid	674.38	914.42	51.35	433	0.2924	0.902
m-coumaric acid	659.82	894.68	49.70	433	0.2893	0.902
p-coumaric acid	656.39	890.01	48.09	433	0.2814	0.902

Table 4. Estimated vapor pressure and molar volume of *o*-, *m*-, and *p*-coumaric acids

Solute	T [K]	Molar volume [cm^3/mol]	Vapor pressure ×10^9 [bar]
o-coumaric acid	308.15	87.527	0.3292
	313.15	87.126	0.6919
	323.15	86.612	2.8255
m-coumaric acid	308.15	87.944	0.8693
	313.15	87.668	1.1790
	323.15	87.378	7.0271
p-coumaric acid	308.15	87.386	1.1001
	313.15	87.141	2.2556
	323.15	86.905	8.7729

3. SCF Solubility Correlation by a Lattice EOS

To model the solubility of coumaric acid isomers, a new equation of state (EOS), developed recently by the present authors and which is based on the nonrandom lattice-hole theory was utilized [Lee and Yoo, 1997]. The final expression of the EOS is written for a general mixture as:

$$P=\frac{1}{\beta V_H}\left\{\frac{z}{2}\ln\left[1+\left(\frac{q_M}{r_M}-1\right)\rho\right]-\ln(1-\rho)\right.$$
$$\left.+\frac{z}{2}\sum_{i=1}^{c}\theta_i\left(\frac{\tau_{0i}}{\sum_{k=0}^{c}\theta_k\tau_{ki}}-1\right)\right\} \tag{2}$$

$$\tau_{ji}=\exp\{\beta(\varepsilon_{ji}-\varepsilon_{ii})\}; \tag{3}$$

where, $q_M=\Sigma x_iq_i$, $r_M=\Sigma x_ir_i$, $\rho_i=N_ir_i/N_r$, $\rho=\Sigma\rho_i$ and x_j is the mole fraction of species i. We set the coordination number (z) at 10 and the unit lattice cell volume, (V_H) at 9.75 cm^{3}mol^{-1}. Other expressions such as chemical potential necessary for phase equilibria calculation are omitted here [Lee and Yoo, 1997]. If we set the subscripts i=1 and j=0, Eq. (2), the EOS is reduced specific for a pure fluid expression.

The two molecular parameters in the EOS for pure fluids; V_1^* and ε_{11} were determined from the estimated molar volumes and vapor pressures of pure components [Lyman et al., 1990], and they were fitted by the following empirical expressions.

$$\varepsilon_{11}/k=E_a+E_b(T-T_0)+E_c(T\ln T/T_0+T-T_0) \tag{4}$$

$$V_1^*=V_a+V_b(T-T_0)+V_c(T\ln T/T_0+T-T_0); \tag{5}$$

where the reference temperature, T_0 is 273.15 K.

The estimated values for the coefficients in Eqs. (4) and (5) are summarized in Table 5 for CO$_2$ and coumaric acid

Table 5. Coefficients of EOS parameter correlations given by Eq. (4) and (5)

Component	E_a	E_b	E_c	V_a	V_b	V_c
carbon dioxide	85.91302	−.10298	−.36562	34.28608	.01428	−.01304
o-coumaric acid	93.12624	.49317	1.52263	35.17175	−.09509	−.82204
m-coumaric acid	93.02592	.48259	1.36263	34.68397	−.05948	−.54833
p-coumaric acid	91.74731	.50051	1.66029	35.69325	−.06975	−.68429

Table 6. Best-fitted binary interaction energy parameters given by Eq. (6)

	$\lambda_{12}^{(0)}$	$\lambda_{12}^{(1)}\times 10^3$
CO_2/*o*-coumaric acid	−1.81186	1.47300
CO_2/*m*-coumaric acid	−1.60072	.894499
CO_2/*p*-coumaric acid	−1.85377	1.97150

isomers.

For a 1-2 binary mixture, the cross interaction energy, ε_{12} in the EOS is based on the combining rule defined by

$$\varepsilon_{12}=(\varepsilon_{11}\varepsilon_{22})^{0.5}(1-\lambda_{12}^{(0)}-\lambda_{12}^{(1)}T); \qquad (6)$$

where the temperature-dependent binary adjustable parameters, $\lambda_{12}^{(0)}$ and $\lambda_{12}^{(1)}$ were empirically fitted using the experimental data for isomeric coumaric acid/CO_2 systems, and are summarized in Table 6.

RESULTS AND DISCUSSION

The solubility (y_2) of *o*-, *m*- and *p*-coumaric acid in CO_2 was measured at 308.15, 313.15 and 323.15 K. The measured pressures at each isotherm were varied by 8.5, 10, 15, 20, and 25 MPa, respectively. The measured data are summarized in Table 7. According to the experimental results, we found that *m*-coumaric acid shows the highest solubility in CO_2 among the isomers. Also, *o*- and *p*-coumaric acids showed similarly low solubility. For each coumaric acid, solubility tends to increase with increasing temperature and pressure, and drastically increased in the supercritical region of the critical pressure of carbon dioxide.

Since we cannot find similar data in literature, we could not compare the data obtained in this work with other data sources. Instead, we performed measurements at least three times for each temperature and pressure to increase the reliability of the data.

Table 7. Measured solubility of *o*-, *m*-, and *p*-coumaric acids in carbon dioxide

T [K]	P [MPa]	Mole fraction, $y_2\times 10^7$		
		o-coumaric acid	*m*-coumaric acid	*p*-coumaric acid
308.15	8.5	0.3165	0.9224	0.3378
	10.	0.4631	1.5318	0.5788
	15.	0.8593	2.8270	1.0798
	20.	1.4763	3.7594	1.6450
	25.	1.9607	5.3383	1.7593
313.15	8.5	0.1107	0.3003	0.1092
	10.	0.3944	1.0197	0.2640
	15.	1.1720	3.0237	1.1818
	20.	1.7046	5.0175	2.2530
	25.	2.7764	7.2540	2.9437
323.15	8.5	0.0185	0.01653	0.0616
	10.	0.1359	0.51463	0.0856
	15.	1.7921	5.2357	1.7727
	20.	2.5390	7.1503	2.8027
	25.	3.8984	13.320	3.5045

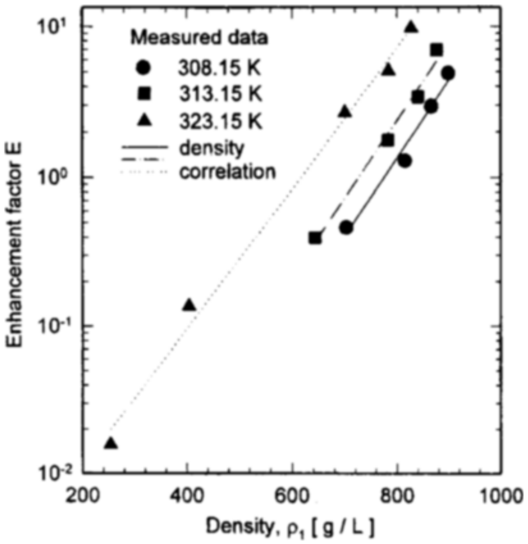

Fig. 2. Measured solubility enhancement of *o*-coumaric acid by the density model-based correlation.

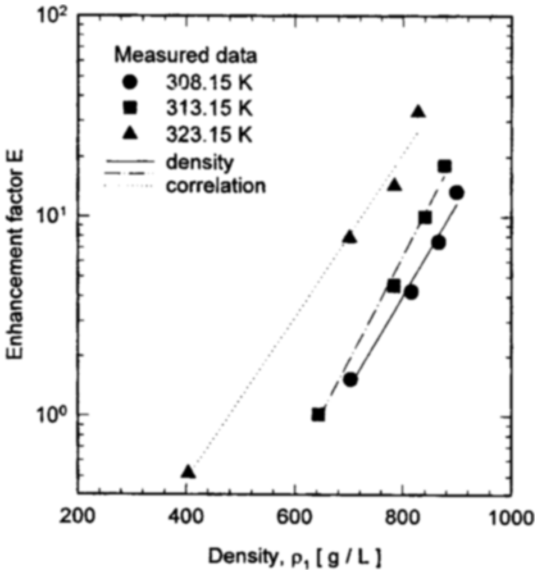

Fig. 3. Measured solubility enhancement of *m*-coumaric acid by the density model-based correlation.

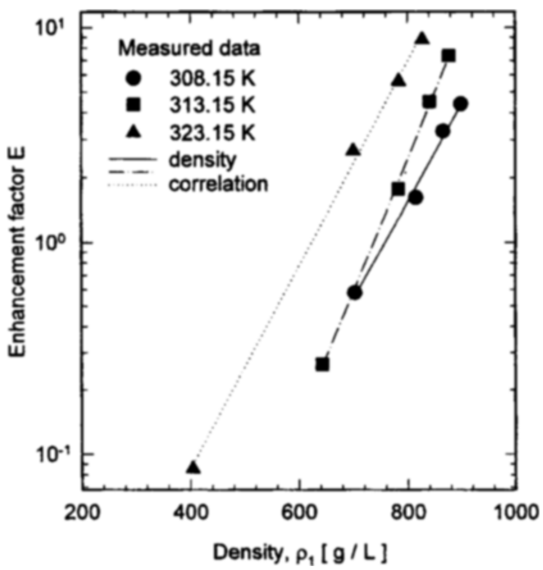

Fig. 4. Measured solubility enhancement of *p*-coumaric acid by the density model-based correlation.

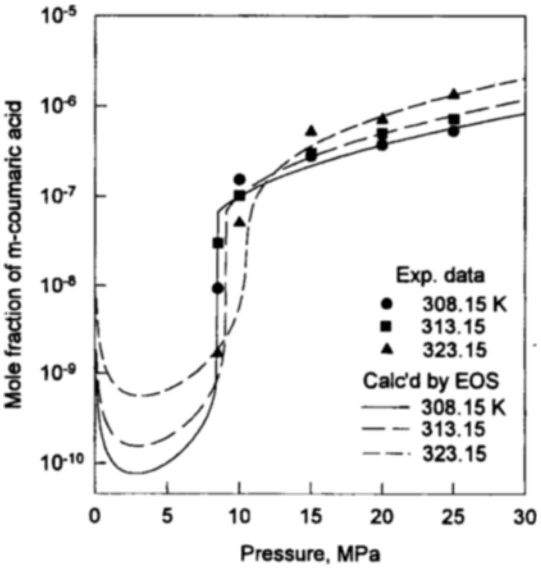

Fig. 6. Measured solubility of *m*-coumaric acid and correlation by the lattice EOS.

The correlated results of Eq. (1) for *o*-, *m*- and *p*-coumaric acids is shown in Figs. 2-4, respectively. When we define a complete linearity of the fitted results as $r^2=1$, the correlation showed average linearity from $r^2=0.98-0.99$, with an average fitting error of 8.99-16.21 % when the density model-based correlation is employed [Giddings et al., 1969]. When we use this type of empirical correlation, the qualitative behavior of the solubility enhancement factor (E) can easily be evaluated. However, we cannot extend these correlation results outside the region of the experimental temperature and pressure. We also attempted to correlate the experiment using the quantitative EOS, which has a sound theoretical basis.

Based on the EOS parameter information provided by Tables 5 and 6, the measured solubility of coumaric acids were correlated by the lattice EOS and the correlation results are shown in Figs. 5-7 for *o*-, *m*- and *p*-coumaric acid, respectively. In Fig. 5, the measured and calculated effect of supercritical temperature and pressure on the solubility of *o*-coumaric acid in CO_2 are shown. We found that the o-coumaric acid dissolved well into CO_2 with increasing temperature and pressure. Also there exists a phenomenon of crossover of solubility behaviors in the region of pressure of approximately 10 MPa. For the cases of *m*- and *p*-coumaric acid, similar solubility behaviors tended to increase with increasing pressure (Figs. 6 and 7). Since the measured phase equilibria of coumaric acids in supercritical CO_2 found to be highly non-ideal, it was necessary to employ different binary adjustable parameter, λ_{ij} for each isotherm in order to fit quantitatively the measured data by the EOS. Thus, we employed a single value of temperature-dependent binary interaction energy param-

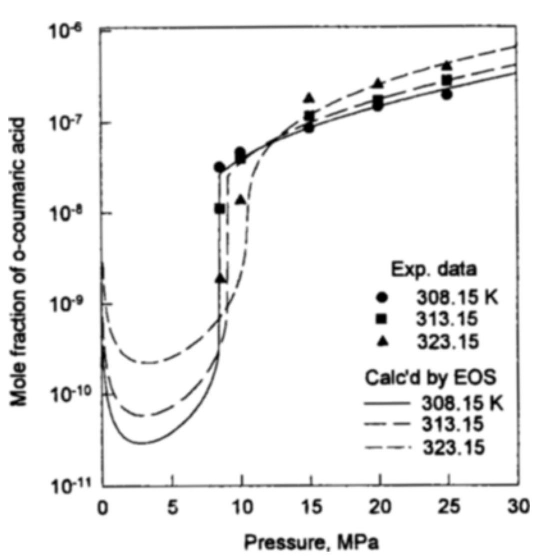

Fig. 5. Measured solubility of *o*-coumaric acid and correlation by the lattice EOS.

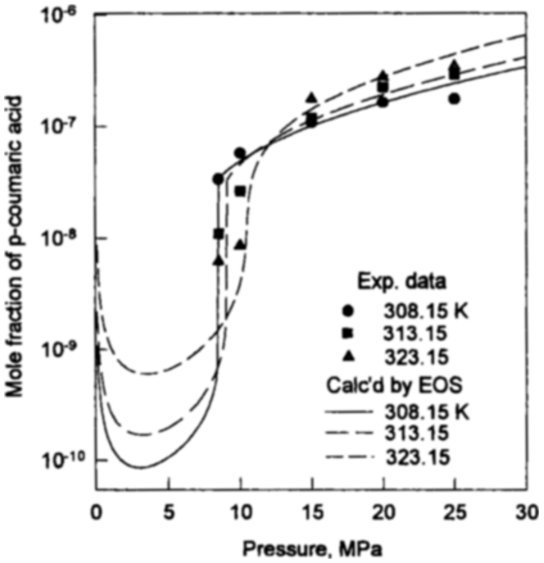

Fig. 7. Measured solubility of *p*-coumaric acid and correlation by the lattice EOS.

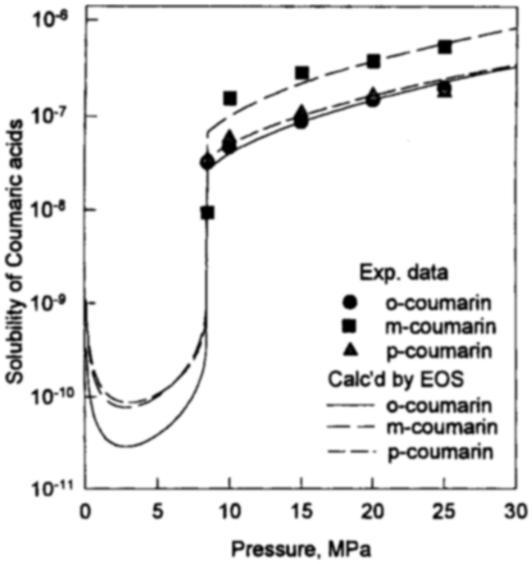

Fig. 8. Isothermal solubility behavior of *o*-, *m*- and *p*-coumaric acids in CO_2 at 308.15 K.

eter, $\lambda_{ij}(T)$. As a result, it was possible to correlate the experimental data in a quantitative manner for the purpose of process design.

Finally in Fig. 8, the isothermal solubility behavior of *o*-, *m*-, and *p*-coumaric acids in carbon dioxide at 308.15 K is shown. As one can see, *m*-coumaric acid dissolves more in carbon dioxide than *o*- and *p*-coumaric acids.

CONCLUSION

The solubility of *o*-, *m*- and *p*-coumaric acids in supercritical carbon dioxide were measured by a flow type phase equilibrium apparatus. Qualitative and quantitative thermodynamic modeling of the solubility data were conducted by utilizing an empirical density model-based correlation and the EOS recently formulated by one of the present authors. We believe that the two types of the thermodynamic modeling approaches can be reliably extended to other mixtures containing biomolecular species.

ACKNOWLEDGMENT

The authors are grateful to the Korea Science and Engineering Foundation for financial support.

REFERENCES

Casteele, K. V., Geiger, H. and Sumere, C. E. V., "Separation of Phenols and Coumarins by Reverse-Phase HPLC", *J. Chromatogr.,* **258**, 111 (1983).

Choi, Y. H., Kim, J. W., Noh, M. J., Park, E. M. and Yoo, K.-P., "Extraction of Epicuticular Wax and Nonacosan-10-ol from Ephedra Herb Utilizing Supercritical Carbon Dioxide", *Kor. J. of Chem. Eng.,* **13**, 216 (1996).

Giddings, J. C., Myers, M. N. and King, J. W., "Dense Gas Chromatography at Pressures to 2000 Atmosphere", *J. Chromatogr. Sci.,* **7**, 276 (1996).

Lee, C. S. and Yoo, K.-P., "Lattice-Hole Based Equations of State and Their Applications to Complex Fluids", Proc. Int. Symp. on Molec. Thermo. and Molec. Simul., No. 109, 53, Jan. 12-15, Hosei Univ., Tokyo Japan (1997).

Li, S., Varadarajan, G. S. and Hartland, S., "Solubilities of Therbromine and Caffeine in Supercritical Carbon Dioxide: Correlation with Density-Based Model", *Fluid Phase Equil.,* **68**, 263 (1991).

Lyman, W. J., Reehl, W. F. and Rosenblatt, D. H., "Handbook of Chemical Property Estimation Methods", ACS Press, Washington DC, Ch. 2 (1990).

Noh, M. J., Choi, E. S., Yoo, K.-P., Choi, Y. H., Yeo, H., Lee, J., Park, E. J., Kim, J. W., Park, H. K. and Kim, K. H., "Selective Extraction of Bioactive Substances from Natural Medicinal Resources Utilizing Supercritical Fluid Technology", *Korean J. of Chem. Ind. & Tech.,* **15**, 14 (1997).

Reid, R. C., Prausnitz, J. M. and Poling, B. E., "The Properties of Gases and Liquids", 4th ed., McGraw-Hill Book, Co., Ch. 2&7 (1987).

Skerget, M., Knet, Z. and Habulin, M., "Solubility of Beta-Carotene and Oleic Acid in Dense Carbon Dioxide and Data Correlation by a Density Based Model", *Fluid Phase Equil.,* **109**, 131 (1995).